The Influence of Plasma Shaping on the Damping of Toroidal Alfvén Eigenmodes

ITPA Group on Energetic Particles (email: guenter@ipp.mpg.de) D. Borba[1,2], A. Fasoli[3], N.N. Gorelenkov[4], S. Günter, [5],Ph. Lauber[5], N. Mellet[3,6], R. Nazikian[4] , T. Panis[3], S.D. Pinches[7], D. Spong[8], D. Testa[3] and JET-EFDA contributors*

[1] EFDA CSU Garching, Boltzmannstr. 2, 85748 Garching bei München Germany
[2]Associação EURATOM/IST, Instituto de Plasmas e Fusão Nuclear -Laboratorio Associado, Instituto Superior Tecnico, 1049-001 Lisboa, Portugal
[3] Centre de Recherches en Physique des Plasmas, Association EURATOM -Confédération Suisse, CH
[4] Princeton Plasma Physics Laboratory, Princeton University, USA
[5] Max-Planck-Institut für Plasmaphysik, EURATOM-Association, Garching, Germany
[6] Association Euratom CEA, Cadarache, Saint-Paul-lez-Durance, France
[7] EURATOM/CCFE Fusion Association, Culham Science Centre, Abingdon, OX14 3DB, UK
[8] Oak Ridge National Laboratory, Fusion Energy Theory Group, Oak Ridge, USA
* See the Appendix of F. Romanelli et al., paper OV/1-3, this conference

Abstract. The dependence of the damping of toroidal Alfven Eigenmodes (TAEs) on various plasma parameters and shapes is analysed with numerical models ranging from perturbative MHD codes like CASTOR-K and NOVA-K, via a warm dielectric tensor model like LEMan to gyrofluid (TAEFL) and linear gyrokinetic codes (LIGKA). Joint European Torus (JET) well diagnosed discharges are used to compare the theoretical models against the experiment. The measurement of TAE damping rates by active in-vessel antennas at JET allows for a direct comparison of both frequency and damping rate with theory.

1. Introduction

The successful operation of a Tokamak based Fusion Power Plant relies on the good confinement of the charged fusion products, the alpha particles. Anomalous losses of fast ions will reduce the operational margins and can cause damage to the first wall components. Therefore, the study of fast ion driven collective instabilities is of paramount importance for the successful operation of a Tokamak burning plasma. Since, it is expected that under these conditions the alpha particle velocity is similar to the Alfvén velocity, the Alfvén waves and related instabilities in Tokamaks have been the subject of many studies[1, 2, 3, 21]. Nevertheless, there are a number of aspects that remain unclear and require further analysis before the predictive capability of the present models is sufficiently accurate. A key factor in determining the stability of Alfvén eigenmodes is the damping, and various experiments have been carried out to address this issue, together with developments in theory and computer simulations. Measurements of the damping characteristics on Toroidicity induced Alfvén Eigenmodes (TAE) modes in Ohmic plasmas using active excitation antennae is one of the most effective techniques used to study the details of the damping mechanisms, therefore, allowing the assessment of the different models via direct comparison of the damping model predications and experimental results. The direct measurements of TAE damping using active excitation antennae was performed for the first time in JET [4] and later extended to higher toroidal mode numbers $n > 2$ in JET [6] and Alcator C-mod [5]. These latest measurements performed at JET have triggered the possibility to compare the different models developed for the damping of Alfven Eigenmodes for higher mode number, i.e. the most relevant mode number concerning the destabilisation by fast ions.

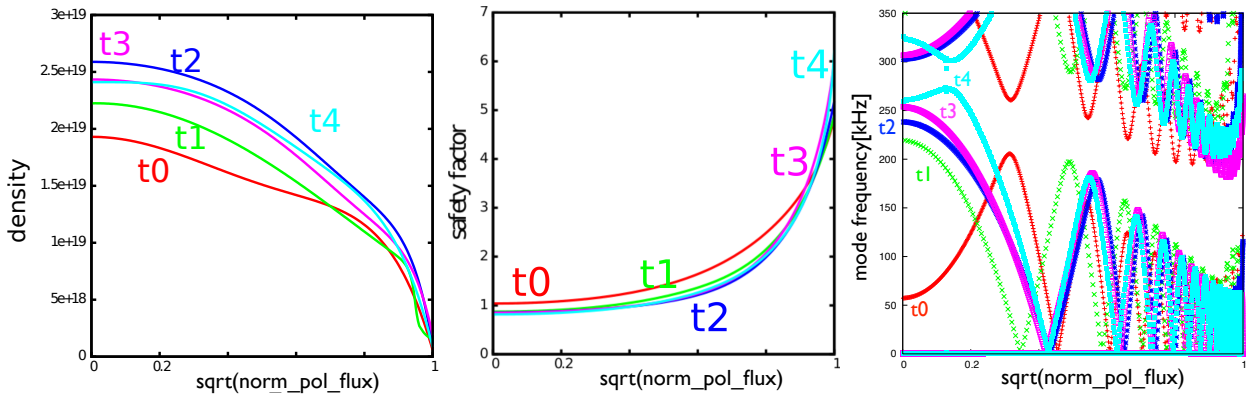

FIG. 1: Density profiles, q-profiles and the shear Alfvén continuum for the time points t_0 to t_4

The JET equilibrium profiles were used as a platform for code to code comparisons, based on the experimental results obtained in discharge #77788 as described in [6]. Parameter scans in well diagnosed discharges are a very promising way to benchmark and validate the theoretical and numerical models against the experiment. A series of equilibria was carefully reconstructed forming the basis for both a detailed physics analysis of the effect of q-profile relaxation and shaping on the TAE stability as well as a world-wide code benchmark. The models range from perturbative MHD codes like CASTOR-K and NOVA-K, via a warm dielectric tensor model like LEMan to gyro fluid (TAEFL) and linear gyrokinetic codes (LIGKA). After documenting the code-code comparisons in detail, the limits and caveats of comparing the simulation results to the experiment are discussed. Also the coupling between the vacuum region and the plasma is adressed.

2. Equilibrium Reconstruction, Theoretical Models and Numerical Implementations

As the basis of the numerical damping calculations, a series of numerical equilbria were generated for JET discharge #77788 at the following times: $t_0 = 4.9895$s, $t_1 = 6.144$s, $t_2 = 10.157$s, $t_3 = 14.139$s and $t_4 = 15.835$s. The first and last of these time points were constrained using polarimetry measurements, whilst the three intermediate points were constrained using MSE measurements made possible by short (250 ms) beam blips (1.5 MW). The electron density and temperature profiles where provided by the high resolution Thomson scattering diagnostic, whilst the ion temperature was provided by charge exchange measurements and shows that $T_e = T_i$. As can bee seen in figure 1 the q-profile in the plasma centre and the density evolve slightly till $t_2 = 10s$, whereas for $t > 10s$ just q_{edge} increases as a consequence of the increasing elongation (see fig. 3a). The temperature profile stays relatively constant within the considered time interval. All equilibria and profiles are available on the ITPA web page (http://itpa.ipp.mpg.de).

2.1. CASTOR-K

The hybrid MHD-kinetic CASTOR [7, 8] model solves the linearized resistive MHD equations in toroidal geometry, where the finite Larmor radius effects and the effect of the parallel electric field are included in the model within the complex resistivity approximation [9, 10]. The CASTOR-K code calculates the non-ideal Alfvén spectrum using two distinct numerical algorithms. In the first procedure the linearized non-ideal MHD equations are solved as an eigenvalue problem using inverse vector interaction. In the second method the plasma response to an external antenna excitation is calculated using a linear solver. The damping of the eigen-

mode is determined by the width of the resonance or directly from the eigenvalue. Numerical convergence for a JET limiter Ohmic discharge requires around 151 radial finite cubic elements and $11-17$ poloidal Fourier harmonics, depending on edge q and toroidal mode number of the eigenmode. For the n=3 case considered here, (#77788) 301 radial finite cubic elements and 17 poloidal Fourier harmonics were used.

2.2. LEMan

The LEMan [11, 12] code is a full-wave direct solver of the Maxwell's equations. Those are written in terms of potentials in order to avoid the so-called numerical pollution, and under the assumption that the Colomb Gauge is satisfied. The warm model is implemented through the dielectric tensor where only terms of the zeroth order in the Finite Larmor Radius (FLR) expansion are retained. In the Alfvén frequencies domain, the convolution method used in LEMan computes the solution of this problem by considering the exact expression of the parallel wave vector. A precise evaluation of this term is crucial as it strongly affects the wave propagation and damping. From a numerical point of view, the solution is discretized as a Fourier series for the poloidal and toroidal angles and as Hermite cubics finite element in the radial direction. The numerical scheme corresponds to a weak Galerkin form. LEMan uses three-dimensional equilibria computed from VMEC [13] that are mapped into the Boozer coordinate by the TERPSICHORE [14] code. The latter retains presently the up-down symmetry and does not allow LEMan to take into account such asymmetry that appears, for example, in the presence of an X-point.

2.3. LIGKA

LIGKA[15] is a linear gyrokinetic eigenvalue code based on the model of Qin,Tang and Rewoldt [16]. It has been extended in several aspects, most importantly with respect to the inclusion of realistic geometry (non up-down symmetric) and low-frequency physics [17]. Second order FLR effects are retained in order to decscribe the mode conversion to kinetic Alfven waves. By employing the HAGIS code [18] for the particle orbits (both electrons and background ions), finite orbit width effects in realistic geometry are accounted for. For this paper the antenna-version of LIGKA was employed: scanning the frequency results in a response spectrum that allows one to determine the damping rate via measuring the full width at half maximum (FWHM) of the response peaks. It should be noted, that this model does not include a proper vacuum region. Therefore, a direct comparison to the experimental situation (TAE antenna) is not entirely valid. However, calculations with the CASTOR-K code presented below give a clear estimate about the uncertainties due to this simplification. For this JET $n = 3$-TAE case, 19 poloidal harmonics $(-1, ..., 17)$ are kept. The radial grid consists of 384 equidistant grid points.

2.4. NOVA-K

NOVA suite of codes are linear hybrid MHD/kinetic codes for EP driven ideal and kinetic MHD eigenmode instabilities. NOVA solves ideal MHD equations and finds eigenmodes, such as TAEs [19]. NOVA-K evaluates fixed mode TAE kinetic growth rates by employing the quadratic form with the perturbed distribution function coming from the drift kinetic equation [19, 20]. It is able to predict various kinetic growth and damping rates perturbatively, such as the continuum damping, radiative damping, ion/electron Landau damping, fast ion drive and trapped electron collisional damping. NOVA is routinely used for AE structure computations and comparisons with the experimentally observed instabilities [21, 23]. The main limitations

of NOVA codes are caused by neglecting thermal ion FLR, toroidal rotation, and drift effects in the eigenmode equations. Thus NOVA can not reproduce some important modes, such as kTAE, kinetic RSAE modes. Therefore it can not describe well some of the dampings, such as radiative damping. The employed model for the radiative damping is perturbative and is based on the assymptotic theory developed earlier [22]. Continuum damping is also perturbative with the analytic description of the logarithmic singularities near the resonances with the Alfvenic continuum [21]. Finite element methods are used in radial direction and Fourier harmonics are used in poloidal and toroidal directions. In the particular results reported here we used uniform in $\sqrt{\Psi_{pol}}$ grid with 201 and 258 in radial and poloidal directions, and poloidal harmonics ranging from -3 to 20.

2.5. TAEFL

The TAEFL model is a reduced MHD initial value code that uses gyrofluid closure techniques [25, 26] for the energetic ions to incorporate the Landau resonance effects that destabilize Alfvén modes. This model incorporates ion/electron Landau damping, continuum damping and radiative (finite ion FLR) damping effects. It uses Fourier spectral representations in the poloidal and toroidal directions and finite differences in the direction normal to flux surfaces.TAEFL is currently limited to up-down symmetric, but noncircular equilibria; the JET equilibria used in this study were modified to be up-down symmetric, but with similar noncircular shaping with respect to elongation/triangularity. Since TAEFL is an initial value model, only unstable cases can be addressed and damping rates could only be inferred indirectly; several methods were tried, including extrapolation of growth rates to zero drive ($\beta_{fast} = 0$) and comparison of cases with no damping effects to those with damping. In practice, the extrapolation to zero drive method provided the best agreement. The TAEFL simulations of JET used 300-400 radial points and 26 Fourier modes (m = 0 to 25). Prior to the damping evaluation, the initial step was to select fast ion profiles and parameters that would excite an unstable mode of close to the real frequency of the antenna excitation. Damping rates from continuum damping can, in some cases, vary sensitively with the mode frequency so it was important to approximate the driving frequency. While deviations of about a factor of 2 are present between the measured and predicted damping rates, they both follow a similar upward variation in time. While this approach may not be as precise as methods that are more directly targeted to modeling antenna-driven damping, it demonstrates that damping levels can be inferred from time-evolution instability models that are reasonably similar to experimental results.

3. Elongation Scan

Due to the shapes of the density and the safety factor profiles, the gaps in the shear Alfvén (SA) continuum are not aligned (see fig 1) and thus all TAEs at all time points are subject to continuum damping either in the core or at the edge. Furthermore, radiative damping [27] is present within the gaps, that depends mainly on the shear and on the background ion Larmor radius. Other damping mechanisms such as ion and trapped electron collisional damping are small in this case. Whereas the hybrid models can directly separate the radiative contribution from the continuum damping, the gyrokinetic codes can only indirectly estimate these contributions by looking at the absorption (LEMan) or at the electric field that is proportional to the absorption (LIGKA) as a function of radius (fig 4). Therefore, in the table in the appendix for LEMan and LIGKA, all contributions to the overall damping that are not related to the continuum are summariesed under 'radiative damping' for simplicity. Furthermore, in this paper all damping

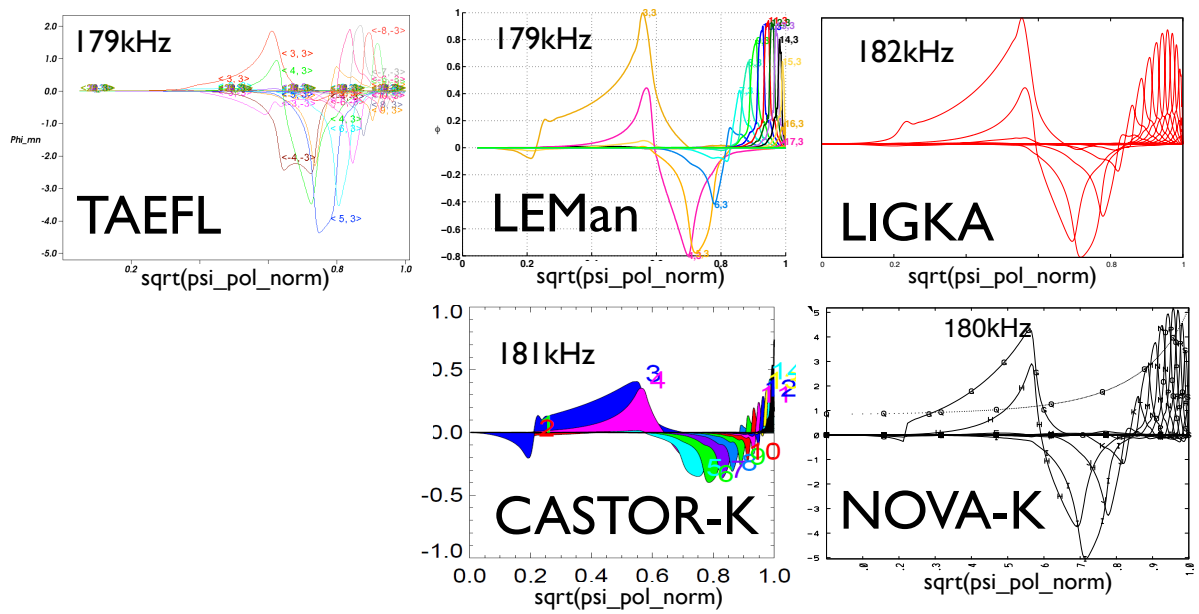

FIG. 2: Eigenfunctions for the least damped TAE mode as calulated by the different codes at t_2. Note that the TAEFL plot also contains the imaginary part, labeled with negative mode numbers.

rates are defined to be positive.
In general, very good agreement for the mode frequencies is found (see tables in the appendix). In most of the cases the eigenfrequencies as calculated by the codes differ by less than $3kHz$ compared to the experimental values. Moreover, all the codes show a very similar localisation, parity and ratio of the poloidal harmonics for the corresponding eigenfunction structure (see fig.2).
The increasing damping with elongation observed in the experiment is also reproduced qualitatively by all the models (fig. 3a), however, the predicted damping rates are typically slightly lower by about factor of $1.5-2$ for most of the codes than those observed in the experiment.

In some cases, such as for the time slice t_1 of shot #77788 a mode with lower damping than the one matching the frequency observed in the experiment ($f = 196$ kHz, $\gamma/\omega = 1.1\%$) is found at $f = 219$kHz by CASTOR-K ($\gamma/\omega = 0.49\%$), LIGKA ($\gamma/\omega = 0.82\%$) and NOVA-K ($\gamma/\omega = 0.47\%$). Also at t_3 NOVA-K ($\gamma/\omega = 1.25\%$) and LIGKA ($\gamma/\omega = 1.5\%$) predict a mode with lower damping at $f \sim 200$ kHz whereas the experiment finds a mode at 176kHz with $\gamma/\omega = 3.7\%$. Simulation of the antenna response for the case at t_1 with CASTOR-K shows that although the damping rate is lower for the mode predicted to exist at $f = 219.0$kHz, the antenna response is also lower on average by a factor of 3, depending on the model for the vacuum and conducting structures around the plasma. This might explain why this mode is not detected in the experiment. Sensitivity studies (see fig. 3b) performed by changing the position of the modeled conducting wall from just behind the antenna (10 cm from the plasma) to the position of the JET Vacuum vessel (28 cm from the plasma) show no significant change in the mode frequency 0.5%. However, a 40% change in the damping of the mode is observed, confirming once more the exponential sensitivity of the mode damping.

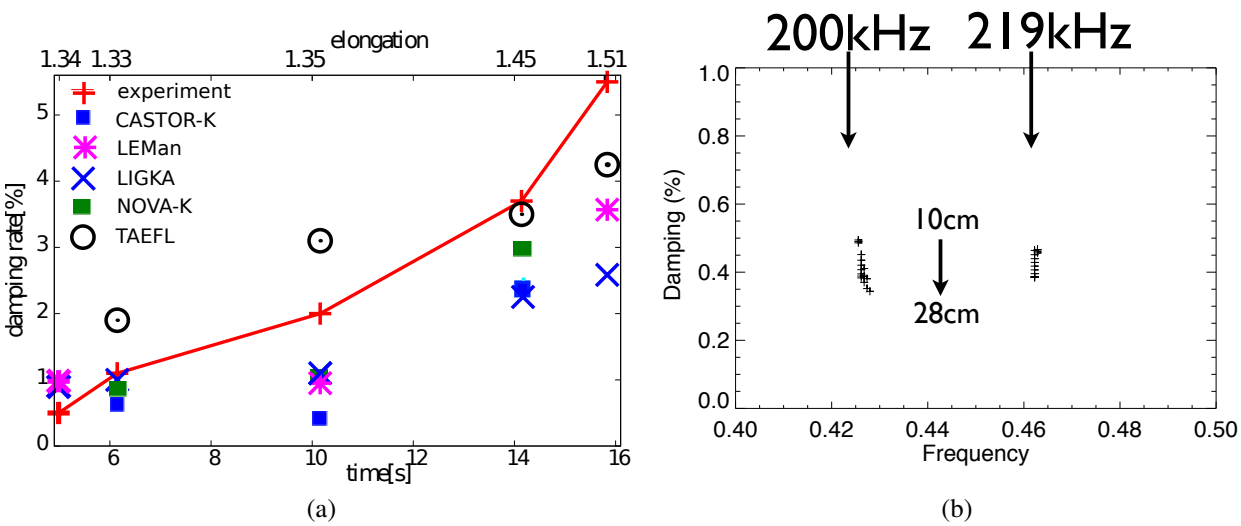

(a) (b)

FIG. 3: Left: damping rates as a function of time and elongation (upper axis). Right: a scan of the distance between the vessel wall and the plasma from 10cm to 28cm with CASTOR-K decreases the damping by $30-40\%$

4. Background Temperature Scan

In order to compare the models for radiative damping, a background temperature scan was carried out for the equilibrium t_2 where radiative damping dominates. The density was kept constant and both ion and electron temperature profiles were scaled via the on-axis temperature T_0. As can be seen in figure 4, all codes (NOVA-K, LEMan, LIGKA) show the expected trend: a larger gyro-radius increases the coupling or 'tunneling' to the kinetic Alfvén wave resulting in a higher damping for higher temperature. The slighty stronger dependence of the damping on the gyroradius calculated by LIGKA seems to be due to the more complete inclusion of kinetic effects such as second order finite Larmor radius and finite orbit width effects that are missing in the other models. A detailed comparison of LEMan and LIGKA shows the sensitivity of the damping mechanisms with respect to the SA continuum (see figs 4 and 5): the mode frequency found by LEMan (179 kHz) is slightly lower than that of LIGKA (182kHz). Therefore, the radiative damping in the outer gaps (large shear) is larger for LIGKA (see fig. 4, right) since the mode is closer to the SA continuum. In the central gap ($\rho = 0.55$) the damping is almost equal although the mode found by LIGKA is further away from the SA accumulation point. As discussed above, this is due to the different FLR models. The difference in the damping for the mode at ~ 200 kHz seems to be correlated with the edge model: whereas LIGKA (1.25%) and NOVA-K (0.6%) predict a rather moderate damping, LEMan, the only code with a proper plasma vacuum interface, calculates a much higher damping (2%) . Therefore, one can conclude that especially when the mode couples through the continuum at the edge, the vacuum-plasma interface model becomes important.

5. Summary and Conclusions

This benchmark and validation exercise shows that both hybrid codes and self consistent gyrokinetic/gyrofluid codes produce relatively similar results for the damping of $n = 3$ TAE modes. The more robust features such as eigenfrequency and mode structure are in excellent agreement. The discrepancies can be explained by differences in the models, such as for the plasma-

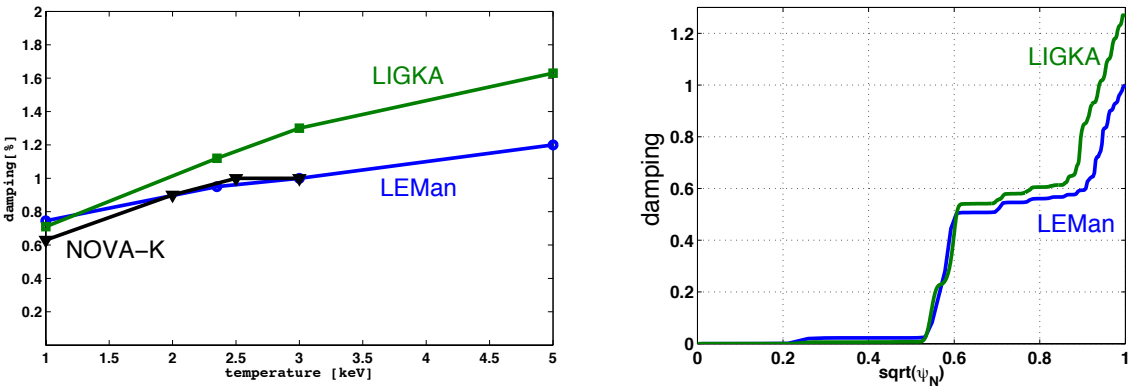

FIG. 4: Mode damping at t_2 as a function of the background temperature (left) and the radial absorption as calculated by LEMan and LIGKA for $T_0 = 2.35keV$ (right). The radial absorption profile is normalised to the LEMan result $\gamma/\omega = 0.95\%$.

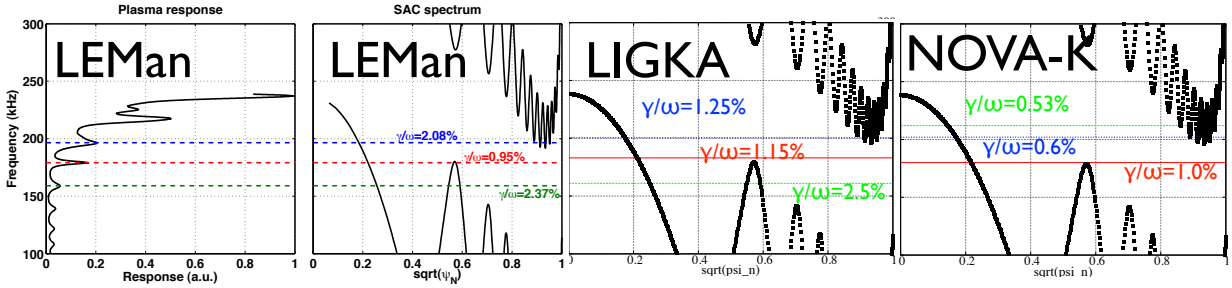

FIG. 5: Antenna scan throughout the gap region by LEMAN and LIGKA for $T_0 = 2.35keV$ (t_2); for comparison also the results obtained with NOVA-K (eigenmodes, no antenna excitation)

vacuum/wall interface and the treatment of background kinetic effects.
Experimental trends (here an elongation scan) can be reproduced by all models remarkably well. Further sensitivity scans with respect to the density and q-profile were carried out (presented elsewhere) showing that within the experimental uncertainties the numerical models are in quantitative agreement with the experimental results.
Finally, the antenna seems to excite modes that couple very well to the plasma edge via an open gap at the edge. However, according to the codes, these antenna-driven modes are not necessarily those with the least damping. This finding is expected to be even more pronounced when more core localised TAEs with higher mode numbers -as expected in ITER- are considered. The implications for the overall energetic ion transport in ITER have to be investigated further.

This work was supported by EURATOM and carried out within the framework of the European Fusion Development Agreement. The views and opinions expressed herein do not necessarily reflect those of the European Commission.

6. Appendix

time point 6.144s (t1); experimental: $196kHz, 1.1\%$				
code	ω[kHz]	γ/ω[%]	γ_{cont}/ω[%]	γ_{rad}/ω[%]
CASTOR-K	219 201 180	0.49 0.62 2.20		
LEMan*	195	0.63	0.05	0.63
LIGKA	221 203 179	0.82 0.94 1.40	0.52 0.005	0.30 0.935
NOVA-K	233 218 202	0.5 0.47 0.9	0.5 0.47 0.46e-3	0 0 0.9
TAEFL	216	1.9		

time point 10.157s (t2); experimental: $180kHz, 2.0\%$				
code	ω[kHz]	γ/ω[%]	γ_{cont}/ω[%]	γ_{rad}/ω[%]
CASTOR-K	181	0.36		
LEMan	197 179 159	2.07 0.95 2.3	0.47	0.48
LIGKA	200 182 161	1.25 1.15 2.5	0.01	1.14
NOVA-K	212 201.6 180	0.53 0.6 1.0	0.53 0.6 0.8e-3	0 0 1.0
TAEFL	178.5	3.1		

time point 14.139s (t3); experimental: $174kHz, 3.7\%$				
code	ω[kHz]	γ/ω[%]	γ_{cont}/ω[%]	γ_{rad}/ω[%]
CASTOR-K	177	2.27		
LEMan *	174	2.45	1.0	1.45
LIGKA	199 181 166	1.5 2.2 2.4	2.0	0.2
NOVA-K	194 178	1.25 3.0	0.65 3.0	0.6 0
TAEFL	181	3.5		

* LEMan results with slightly different q-profiles [6]

References

[1] C.Z. Cheng, L. Chen, M.S. Chance, Annals of Physics **161**, 21 (1985)
[2] C.Z. Cheng, M.S. Chance, Phys. Fluids **29**, 11 (1986)
[3] G.Y. Fu, J.W. VanDam, Phys Fluids B **1**, 2404 (1989)
[4] Fasoli A. et al 1995 Phys. Rev. Lett. 75 645
[5] J. A. Snipes, D. Schmittdiel, A. Fasoli, R. S. Granetz, and R. R. Parker, Plasma Phys. Controlled Fusion 46, 611 (2004)
[6] D. Testa et al Nucl. Fusion 50 (2010) 084010
[7] Kerner W. et al 1998 J. Comput. Phys. 142 271,
[8] Huysmans G.T.A. et al 1993 Phys. Fluids B 5 1545
[9] Connor J. et al 1994 21th EPS Proc. vol 18B (part II), p 616
[10] D. Borba et al Nucl. Fusion 42 (2002) 1029-1038
[11] P.Popovich, W.A.Cooper and L.Villard, Comput. Phys. Comm. 175 (2006), 250.
[12] N.Mellet, CRPP-EPFL PhD Thesis; to be submitted for publication.
[13] S.P.Hirshman, Phys. Fluids 26 (1983), 3553.
[14] D.V.Anderson, W.A.Cooper, R.Gruber, S.Merazzi, U.Schwenn, J. Supercomp. Appl. (1990), 4.
[15] Ph. Lauber et al, J. Comp. Phys., **226/1** (2007)
[16] H. Qin, W.M. Tang, G.Rewoldt, Phys. Plasmas **5**, (1998) 1035
[17] Ph. Lauber et al, Plasma Phys. Controlled Fusion, **51** (2009) 124009
[18] Pinches S.D. et al, C. Ph. Comm., **111** (1998)
[19] C.Z. Cheng ,Phys. Reports, **211** (1992) 1
[20] N. N. Gorelenkov and C. Z. Cheng and G. Y. Fu, Phys. Plasmas, **6** (1999) 2802-2807
[21] N. N. Gorelenkov and H. L. Berk and R. V. Budny, Nucl. Fusion, **45** (2005) 226-237
[22] H.L. Berk, R.R. Mett, D.M.Lindberg, Phys.Fluids B, **5** (1993) 3969
[23] M. A. Van Zeeland et al,Phys. Rev. Letters, **97** (2006) 135001-1
[24] N. N. Gorelenkov, Phys. Rev. Letters, **95** (2005) 265003-1
[25] D. A. Spong, B. A. Carreras, and C. L. Hedrick, Phys Fluids B-Plasma 4, 3316 (1992).
[26] D. A. Spong, B. A. Carreras, and C. L. Hedrick, Phys Plasmas 1, 1503 (1994).
[27] R.R. Mett, S.M. Mahajan, Phys. Fluids B **4**, 2885 (1992)